Atacama
Large
Millimeter /
submillimeter
Array

Preliminary Progress Report on the Implementation of the Bandwidth Transfer Technique for High Frequency Observations

ALMA Technical Note Number: 9

Status: FINAL

Prepared by:	**Organization:**	**Date:**
Jennifer Donovan Meyer (NAASC/NRAO)	ALMA	08 August 2014

Atacama Large Millimeter/
Submillimeter Array
Alonso de Córdova 3107
Vitacura - Santiago Chile

CAPABILITIES SUMMARY

To: Takahashi Satoko (JAO), EOC Management

From: Jennifer Donovan Meyer (NAASC)

Date: 08/17/2014

Subject: Bandwidth Switching Progress Report

Reporting JIRA ticket:
http://jira.alma.cl/browse/CSV-3074

Datasets:
~~1 June, uid__A002_X83210a_Xfb, Band 7 (too much phase decorrelation)~~
~~3 June, uid__A002_X833c94_Xf37, Band 8 (too much phase decorrelation)~~
~~19 June, uid__A002_X84bb63_X2df, Band 3, wide FDM (3840) to narrow FDM (3840) (too much phase decorrelation)~~

19 June, **uid__A002_X84bb63_X68**, Band 3, PWV~1.8.
TDM (128) to narrow FDM (3840)

21 June, **uid__A002_X84e1f2_X45**, Band 7, PWV~1.6.
TDM (128) to narrow FDM (3840)

23 June, **uid__A002_X8505d8_X1eae**, Band 9, PWV~0.83.
ICT-331 fix required first.
TDM (128) to narrow FDM (3840)

8 July, **uid__A002_X8658de_X3a4**, Band 9, PWV~0.63.
TDM (128) to narrow FDM (3840), plus
intermediate FDM (3840) to narrow FDM

Motivation:
Calibrating ALMA high frequency observations in Bands 8, 9, and 10 will be limited by the availability of nearby phase calibrators. This will be particularly problematic for narrow band observations (bandwidths less than 300 MHz) at high frequency. Observing with bandwidth switching will enable higher signal-to-noise observations of faint calibrators found closer to the science targets, thus allowing better atmospheric calibration of those targets than bright calibrators at larger distances. This technique involves transferring the phase solutions of faint calibrators observed in wide spectral windows to science targets observed in narrow spectral

windows. Eventually, this technique will be combined with the Band-to-Band (B2B) transfer technique in order to calibrate high frequency, narrow band observations with lower frequency, wide band calibrator observations.

Testing method:
Observe two nearby bright quasars, one with wide spectral windows and one with narrow spectral windows. Apply the phase solutions from the wide window quasar observations to the narrow window quasar observations. In the first three usable data sets (in Bands 3, 7, and 9), we demonstrate that this technique works. In the final Band 9 dataset (X3a4), we add an intermediate resolution FDM window to the observing setup to compare the noise in the final calibrated images, using first the TDM window(s) and second the FDM window for the phase transfer.

Technique demonstration:
In the first three SBs, the script generator is used to make the data reduction script. In each case, it recognized that the observation intended to use bandwidth switching. Some modification of the generated script was necessary, and the changes are summarized in the following section. The images resulting from these demonstration reductions are shown in Figures 1, 2, and 3.

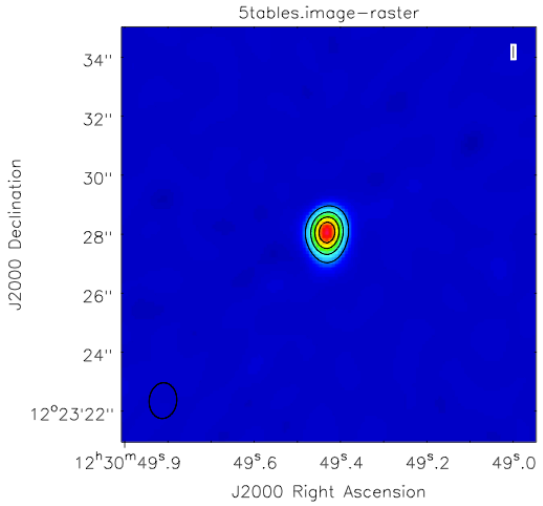

Figure 1: Image of 3C274 in four 58.6 MHz (FDM) windows in Band 3 (X68), using phase transfer from four Band 3 TDM windows.

Atacama Large Millimeter/
Submillimeter Array
Alonso de Córdova 3107
Vitacura - Santiago Chile

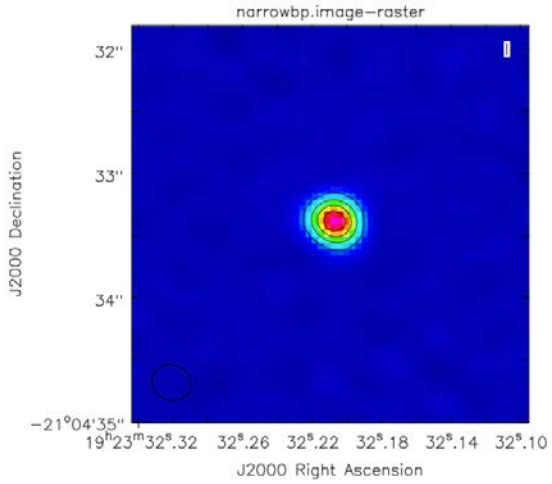

Figure 2: Image of J1923-210 in four 58.6 MHz (FDM) windows in Band 7 (X45), using phase transfer from four Band 7 TDM windows.

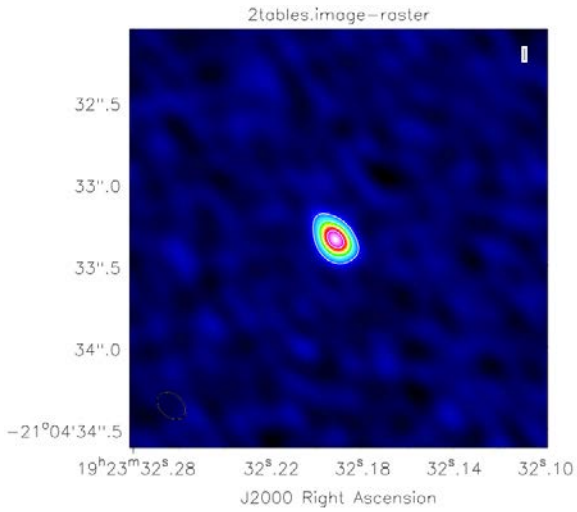

Figure 3: Image of J1923-210 in four 58.6 MHz (FDM) windows in Band 9 (X1eae), using phase transfer from four Band 9 TDM windows.

The observations are set up with four 2 GHz TDM windows and four 58.6 MHz FDM windows. In each case, there is one-to-one correspondence between the TDM and FDM windows; no TDM windows are overlapping. A bright bandpass calibrator is observed in the wide windows (field = '0', spw = '0~3') and in the narrow windows (field = '1', spw = '4~7'), a flux calibrator is observed in the wide windows (field = '2', spw = '0~3'), and then observations of the phase calibrator (field = '3', spw = '0~3') and target (field = '4', spw = '4~7') are alternated until the end of the SB.

Atacama Large Millimeter/
Submillimeter Array
Alonso de Córdova 3107
Vitacura - Santiago Chile

Additions/alterations to the data reduction script:

-- Bandpass. The automatically generated script does not account for the bandpass calibration in the narrow windows; in the bandpass calibration step (12), add a second (solint=int, field=1) gaincal for the narrow window, and set append=True. At band 9 (and likely 10), additional averaging will likely be necessary in both time and frequency, but try to average more in frequency than time. Also create a second call to bandpass for the field=1 source, and specify the spw range in both calls (field=0 and spw=0~3 in the first, and field=1 and spw=4~7 in the second). Add append=True to the second call. These should both be solint=inf, and again in band 9 (and 10) some additional averaging in frequency will likely be necessary.

-- Gain calibration. In the gain calibration step (14), the instrumental phase offsets are determined in the .phase_pre_offsets_inf table with field=0, solint=inf (this table does not need to be changed). The generated spwmap maps the narrow windows to the wide ones:

```
phasemap = range(8)
phasemap[0] = 0
phasemap[1] = 1
phasemap[2] = 2
phasemap[3] = 3
phasemap[4] = 0
phasemap[5] = 1
phasemap[6] = 2
phasemap[7] = 3
```

The second gaincal finds the offset between the wide and narrow windows in the .phase_offsets_inf table; set this to field=1, solint=inf, and add interp = ['', 'linear'], spwmap = [[], phasemap].

The third gaincal corrects the short timescale variability in the wide window calibrators (.phase_int). Remove '1' from the list of fields and add spw='0~3' and set gaintable = ['uid___A002_X84e1f2_X45.ms.split.bandpass', 'file.ms.split.phase_pre_offsets_inf']. I have also been creating a narrow band short timescale variability plot, with field='1', spw='4~7', interp = ['', 'linear'], gaintable = ['file.ms.split.bandpass', 'file.ms.split.phase_pre_offsets_inf', 'file.ms.split.phase_offsets_inf'], spwmap = [[], phasemap, []].

The fourth gaincal sets the amplitude solutions; again split out field = '1' into its own call to gaincal and set append = True. In the field = '0,2,3' call, use gaintable = ['file.ms.split.bandpass', 'file.ms.split.wide.phase_int', 'file.ms.split.phase_pre_offsets_inf']), and in the field = '1' call, use gaintable = ['file.ms.split.bandpass', 'file.ms.split.phase_int', 'file.ms.split.phase_pre_offsets_inf', 'file.ms.split.phase_offsets_inf'], spwmap = [[], [], phasemap, []]). Note that the

reductions described in this document are largely phase calibrations only, but this is how the amplitude calibration would work.

The fifth gaincal sets the long timescale phase variations in the wide window gain calibrator (.phase_inf). Remove '1' from the field list and add spw='0~3'. Here gaintable = ['file.ms.split.bandpass','file.ms.split.phase_pre_offsets_inf']).

-- Applycal.
For the wide window bandpass calibrator (field = '0'), gaintable = ['file.ms.split.bandpass', 'file.ms.split.wide.phase_int', 'file.ms.split.phase_pre_offsets_inf'], gainfield = ['', '0', '0'], spwmap = [[], phasemap, []].

For the narrow window bandpass calibrator (field = '1'), gaintable = ['file.ms.split.bandpass', 'file.ms.split.phase_int','file.ms.split.phase_pre_offsets_inf', 'file.ms.split.phase_offsets_inf'], gainfield = ['1', '1','', ''], spwmap = [[],[], phasemap, []].

For the flux calibrator (field = '2', though I only phase calibrated most of the data shown here), gaintable = ['file.ms.split.bandpass', 'file.ms.split.phase_int', 'file.ms.split.flux_inf', 'file.ms.split.phase_pre_offsets_inf'], gainfield = ['0', '2', '2',''], spwmap = [[], [], [], []].

For the phase calibrator (field = '3'), gaintable = ['file.ms.split.bandpass', 'file.ms.split.phase_inf','file.ms.split.phase_pre_offsets_inf', 'file.ms.split.flux_inf'], gainfield = ['0', '3','', '3'], interp = ['', 'linearPD', '', ''], spwmap = [[], [], [], []].

*Note that interp = 'linearPD' has created some problems; this may need to be changed to interp = 'linear'.

For the science target (field = '4'), gaintable = ['file.ms.split.bandpass', 'file.ms.split.phase_inf', 'file.ms.split.phase_pre_offsets_inf', 'file.ms.split.phase_offsets_inf', 'file.ms.split.flux_inf'], gainfield = ['1', '3', '', '', '3'], interp = ['', 'linearPD', '', '', ''], spwmap = [[], phasemap, phasemap, [], phasemap].

*Note that interp = 'linearPD' has created some problems; this may need to be changed to interp = 'linear'.

A note on interp = 'linearPD': as reported in CAS-6797, adding 'PD' to the interpolation setting leads to (incorrect) residual phase offsets when using phase solutions averaged to the central frequency of an SPW. This is due to the fact that the phase delays are calculated using the frequency at the edge of the SPW. These residual phases are of order 1.5-2 degrees in Band 3, up to 0.5 degree in Band 7, and up to 0.2 degree in Band 9. I have left the phase delay correction in the applycals only for the .phase_inf table applications to fields 3 and 4; with further testing, this

makes very little difference in the rms of the final image (at the 1-2% level), with the 'linearPD' case being marginally worse than the 'linear' case.

Suggestions for changes to the observing setup and observations still needed:
-- As the narrow bandpass calibration is very signal-to-noise limited in the narrowest (62.5 MHz) windows, investigate the possibility of using a solar system object to do the narrow bandpass calibration
-- Currently, the phase offsets between the wide and narrow window are measured using observations of fields 0 and 1, which are generally observed separated by 15-20 minutes. Any change in the atmosphere over this time, which results in more phase offset than is purely instrumental, is therefore included. Adding an additional bandpass calibration (in the wide windows) at the end of the SB, or even immediately following the narrow bandpass observation, to re-measure the phase offset between the wide and narrow window bandpasses will yield an idea of how much phase offset is instrumental and how much is due to changes in the atmosphere.
-- Nagging issues with phase decorrelation (reported in PRTSPR-5946 and ICT-3186) are occasionally seen when switching between FDM and TDM setups (see Figure 4). Turning off scan sequences, an expert mode option, has been identified as a workaround solution. This suggestion was implemented in a successful Band 10 execution during the 8 July EOC week, but the weather was not conducive to high frequency observing. Further testing of this option in the bandwidth switching observations is suggested. In addition, as reported in PRTSIR-3082, this observation caused strange behavior in the numbering of target fields in the imported SB, which is hopefully not related to the scan sequence fix but should also be re-tested.

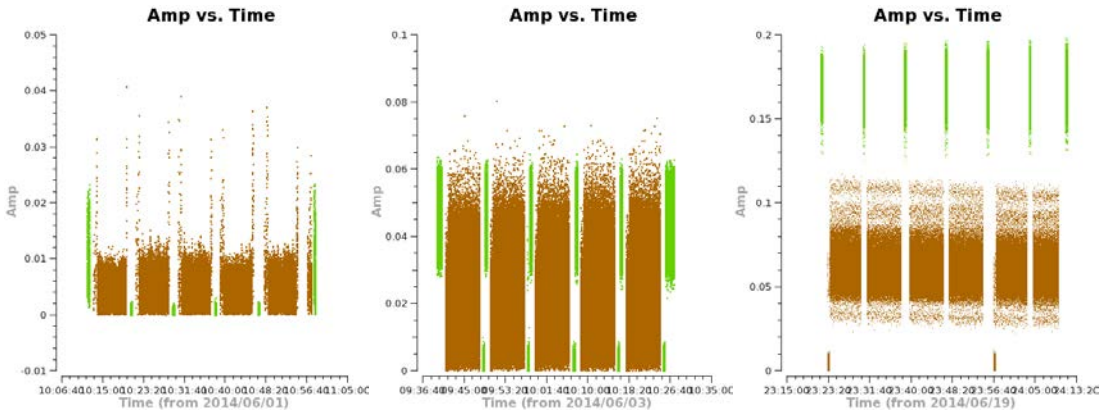

Figure 4: (Left to right) Band 7 (Xfb), Band 8 (Xf37), Band 3 (X68) uncalibrated amplitude vs. time in field 3 (phase calibrator, green) and field 4 (science target, brown). Generally the first 30 seconds – the first few subscans of an observation – are affected. In Xfb, it affects the first and last FDM subscans and the first (all) TDM subscans; in Xf37, it affects the first FDM and TDM subscans; and in X68, it affects the first FDM subscans.

The issue is intermittent in all cases and especially so in X68.

-- In addition to the items listed above, testing observations still needed include: demonstration that this method works in Band 10 (using narrow windows for the science target that are at least 125 or 250 MHz), inclusion of the 7m antennas in the bandwidth switching experiments (since these antennas will be the most signal-to-noise limited at high frequencies) now that the technique has been successfully demonstrated for the 12m array, and observations in varying conditions to test the limits of this calibration method with PWV, width of the narrow bandpass windows, flux of the phase calibrator, and the length of the longest baselines for B9/10.

The necessity of the narrow bandpass measurement:
Since we are signal-to-noise limited in the narrow SPWs at high frequencies, testing is performed to check whether the narrow bandpass correction is really necessary. The results are tabulated in Table 1 below. Specifically, we compare the application of the wide bandwidth bandpass (low frequency resolution) and narrow bandwidth bandpass (high frequency resolution), and in Band 9 we also compare the imaging results using no bandpass correction at all. Since these are only calibrated in phase, the relative results are meaningful and are presented normalized to the narrow bandwidth run. The lack of amplitude calibration may also lead to some bias in the final "no bandpass" case for Band 9. Finally, we test the effect of including the WVR correction in the Band 9 SB (for the median PWV of 0.83).

Table 1: Results of testing the inclusion of the bandpass correction.

	Normalized rms	Normalized peak	Normalized flux density	SNR (peak/rms)
Band 3, wide	1.02	0.99	0.99	163
Band 3, narrow	1.0	1.0	1.0	167
Band 7, wide	1.01	1.0	0.99	124
Band 7, narrow	1.0	1.0	1.0	126
Band 9, wide	0.89	0.91	0.92	29
Band 9, narrow	1.0	1.0	1.0	28
Band 9, no bandpass	0.91	0.93	0.95	28
Band 9, narrow, no WVR	0.81	0.57	0.86	19

In Bands 3 and 7, the narrow bandpass yields a better image of the final calibrator with a lower rms and higher peak/flux density/SNR of the calibrator itself at the 1-2% level.

In Band 9, where we are more signal-to-noise limited, the case is less clear. The rms is better in the wide bandpass (and potentially biased) no bandpass cases, but the phase errors lead to flux being distributed farther from the peak. Here the differences are of order 10%. However, the SNR is very similar in all three cases.

Including the WVR correction increases the rms noise in the final image by 20%, but it does a much better job of recovering flux at the phase center than the "no WVR" case (though in fact, the phase center in the "no WVR" case is closer to the real location of the target; see the section on position offsets below).

The reduction of X3a4:
In the second Band 9 observation, the observing setup includes an intermediate resolution FDM SPW (SPW 4) and an additional high resolution FDM SPW (SPW 5) in addition to the eight usual SPWs (four TDM, SPW 0~3, and four FDM 58.6 MHz wide, SPW 6~9). The central frequencies of the four TDM windows are the same, the frequencies of SPW 5 and 6 are the same, and those of SPW 7 and 8 are the same. The FDM windows are all located within the frequency range of the TDM windows. Phase transfer is applied in this reduction from the wide windows (SPW 0,2), as well as from the intermediate window (SPW 4), to the narrow windows (SPW 5~9). Currently the script generator fails with this type of observation; a script is generated by hand which matches the updates described above. The observation is taken in better weather than the previous Band 9 SB, but the elevation is lower, resulting in an elongated beam shape in the final images. The images with the TDM phase transfer and FDM phase transfer look very similar; the TDM phase transfer image is shown in Figure 5. Transferring phase solutions from the wide TDM windows and intermediate FDM windows does not make much of a difference in the final images; their rms values are very similar.

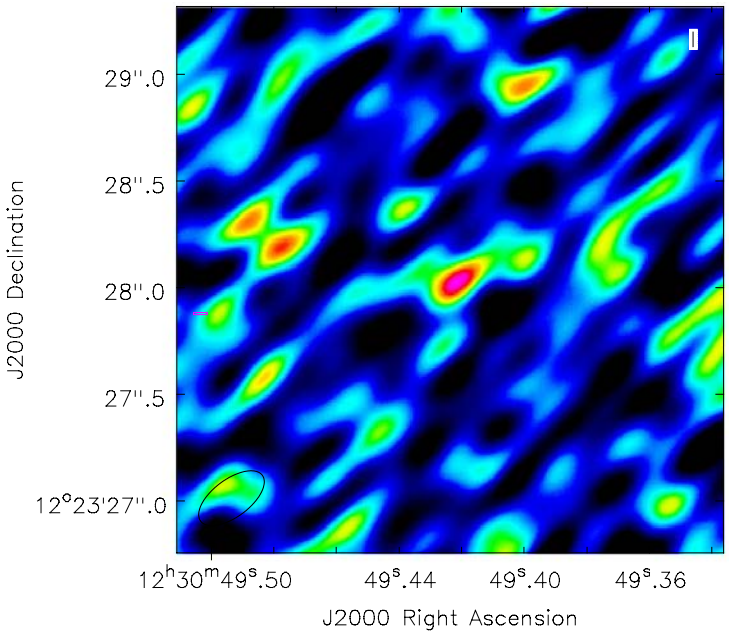

Figure 5: Image of 3C274 in four 58.6 MHz (FDM) windows in Band 9 (X3a4), using phase transfer from one Band 9 TDM window (or one Band 9 intermediate resolution FDM window).

Position offsets when doing bandwidth switching:
In the Band 3 demonstration data, the peak pixel of the science target (a quasar with a known position, which should be located at the phase center) is offset from the phase center by 0.14". The beam size is 1.2"x0.93", so the offset is well less than one beam.

In the Band 7 demonstration data, the peak pixel of the science target is offset from the phase center by 0.28". The beam size is 0.32"x0.28", so the offset is roughly the size of one beam.

In the Band 9 demonstration data, the peak pixel of the science target is offset from the phase center by 0.08". The beam size is 0.19"x0.15", so the offset is roughly half the size of the beam. In the no WVR case, the offset drops to 0.03", less than a quarter of the beam size.

In the Band 9 (X3a4) data, the peak pixel of the science target is offset from the phase center by 0.03" when using a TDM window for the transfer and 0.02" when using the FDM window for the transfer. The beam size is 0.36"x0.18", so the offset is well less than one beam in both cases.

Phase offsets between wide and narrow windows:
Instrumental phase offsets exist between the TDM and FDM windows contained within them. These are measured using the bandpass calibrator observations in both sets of spectral windows. First, the instrumental phase offsets relative to the SPWs of the reference antenna are derived using solint = 'inf' and field = '0' for the wide windows (with the bandpass solutions applied on the fly); this is the .phase_pre_offsets_inf table. Next, the narrow bandpass solutions and wide window instrumental phase offsets table are applied on the fly to the narrow window observation of the bandpass calibrator (field = '1'); the resulting phase residuals, contained in the .phase_offsets_inf table, are the offsets between the wide and narrow windows. There is some atmospheric change that is currently incorporated into these solutions since the two observations of the bandpass calibrator are taken 15-20 mintues apart; in the "suggestions" section, we recommend to take another measurement of the bandpass calibrator later in the SB to quantify how stable the measured offset table is with time.

In Band 3 (X68), the phase offsets between the TDM and FDM windows range from –10 to 10 degrees with a few outliers reaching 20 degrees, and the phase offsets in the two polarizations track each other to within roughly 5 degrees. The four SPWs on each antenna generally vary in the same direction (Figure 6).

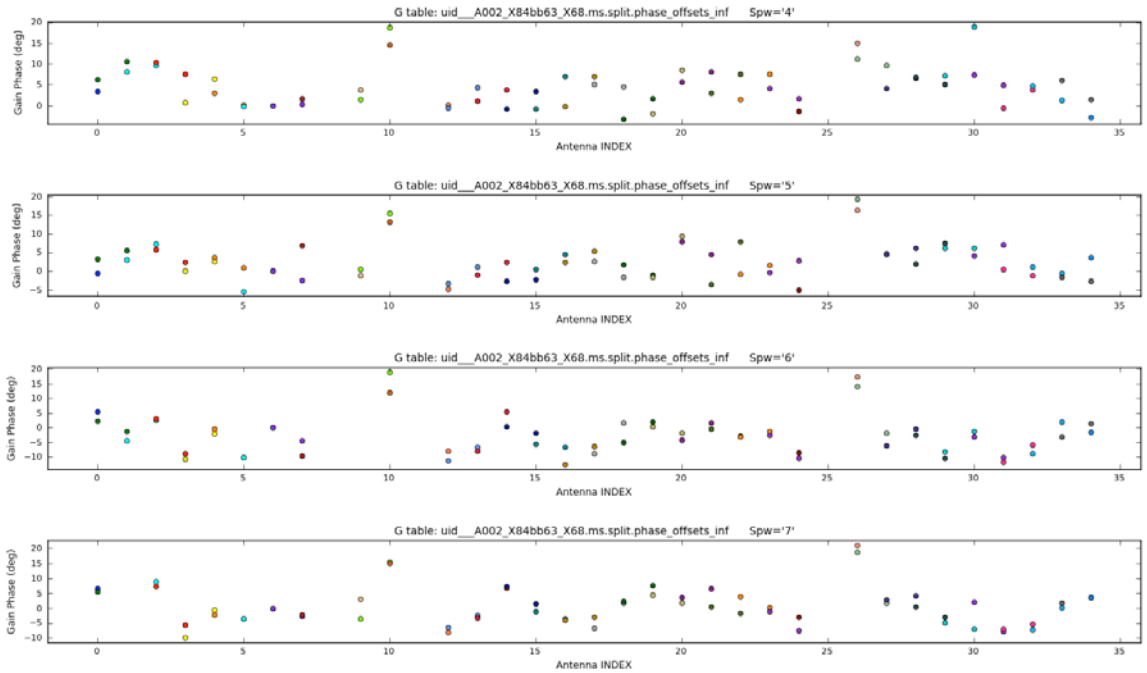

Figure 6: FDM to TDM window phase offsets in Band 3 (X68).

In Band 7 (X45), the phase offsets vary between roughly –50 and 50 degrees, with outliers up to 100 degrees of offset. Again, the two polarizations and four SPWs exhibit fairly consistent behavior to each other (Figure 7).

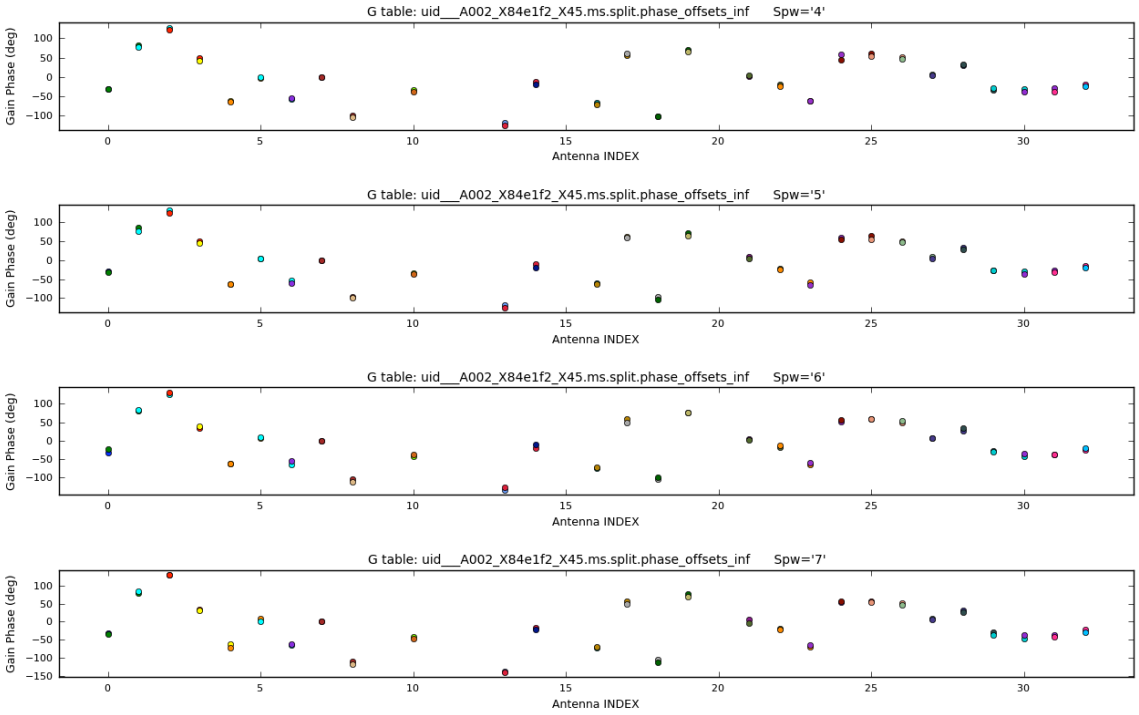

Figure 7: FDM to TDM window phase offsets in Band 7 (X45).

In Band 9 (X1eae), the behavior is similar to Band 7 (X45); the phase offsets generally range between –40 to 40 degrees with only one outlier at larger offset. Here the two polarizations do not track as closely as at the lower frequencies, but their behavior trends in the same direction (with a couple of exceptions that have larger, tens of degrees, of offset between them). The behavior is roughly similar between SPWs (Figure 8). SPW 6 has fewer solutions than the other windows.

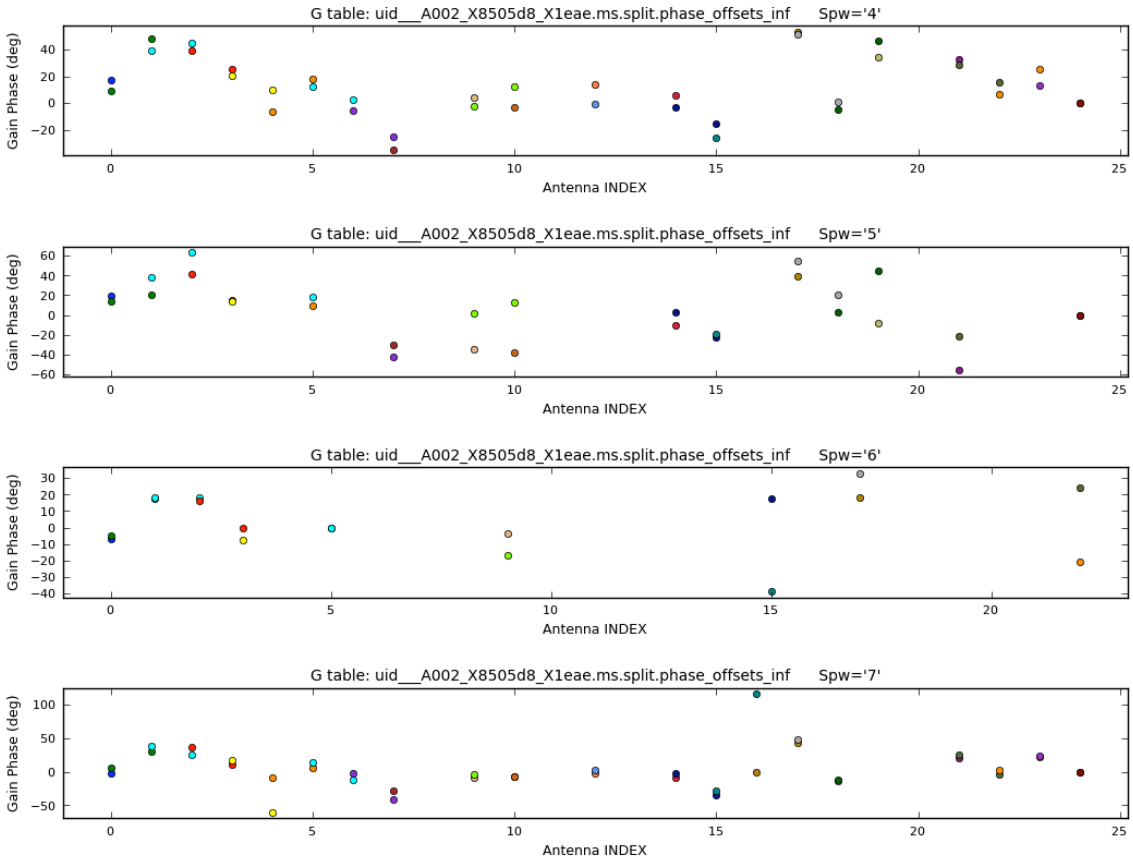

Figure 8: FDM to TDM window phase offsets in Band 9 (X1eae).

To examine the effect of the WVR correction on the phases in the Band 9 SB (X1eae), the same reduction is also run without applying the WVR table. Phase offsets on individual antennas generally change compared to the version of the reduction using WVR, but both versions have similar offset absolute values overall (Figure 9).

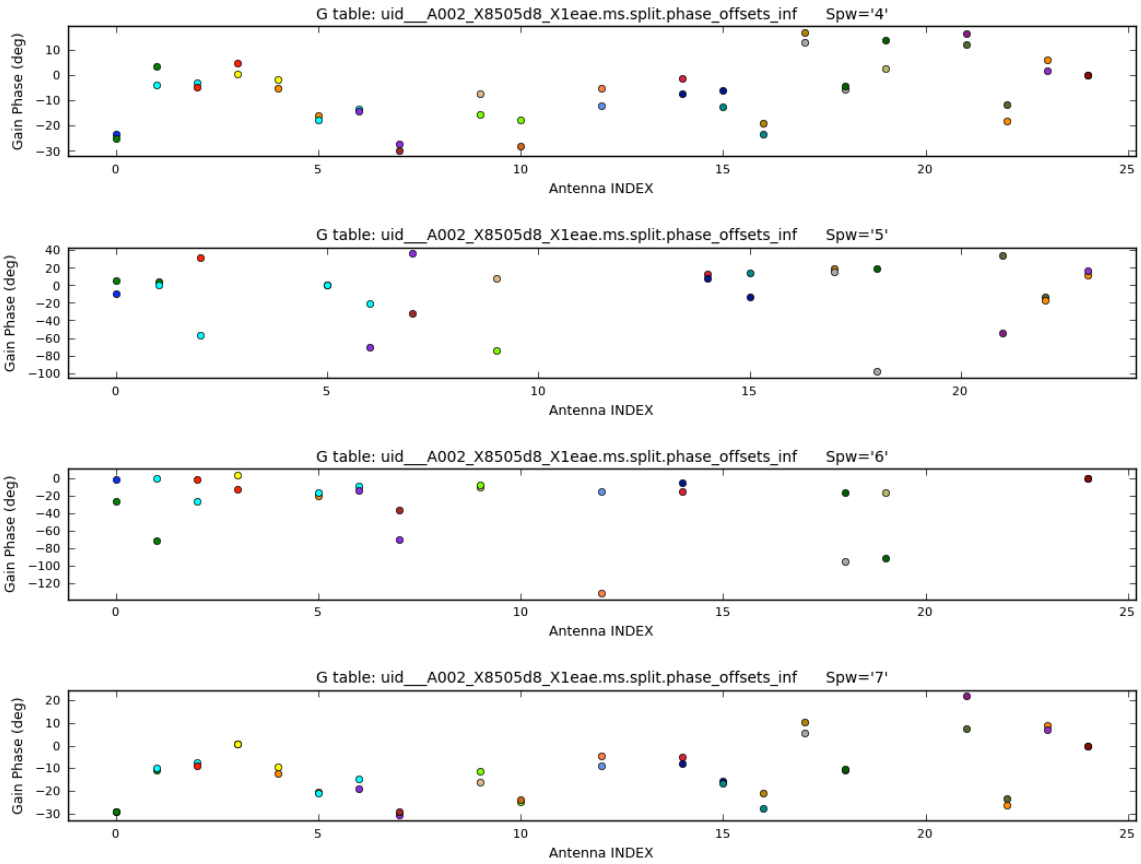

Figure 9: FDM to TDM window phase offsets in Band 9 (X1eae), the same as in Figure 8, with no WVR correction applied.

Finally, we address the phase offsets measured in the second Band 9 SB (X3a4). First, the TDM-to-FDM phase transfer is performed twice using both SPW 0 and SPW 2 as the wide band reference window. Next, the FDM-to-FDM phase transfer is performed using SPW 4 as the reference window. Remember that in this case, all four TDM windows and the intermediate FDM window have (roughly) the same central frequency, and all four narrow FDM windows lie within them.

When using SPW 0 as a reference, the magnitude of the phase offsets in SPW 6 are similar to those seen in B9/X1eae (roughly ranging from –40 to 40 degrees), but the other three SPWs display much larger phase offsets (up to roughly –160/160 degrees). When using SPW 2 as a reference, the same behavior is seen for SPW 8 (offsets are in the range of –40/40 degrees, while the other three SPWs display much larger phase offsets). In the SPW 0/SPW 6 match and in the SPW 2/SPW 8 match, the phase offsets of the two polarizations also tend to agree with each other more than in the other three SPWs, where they differ anywhere from a few degrees to a hundred degrees or more. When looking at the phase offsets relative to the intermediate resolution SPW 4, the findings are similar to those of SPW 0 and SPW

2; here SPW 7 seems to “match” best. These phase offset tables are shown in Figures 10, 11, and 12.

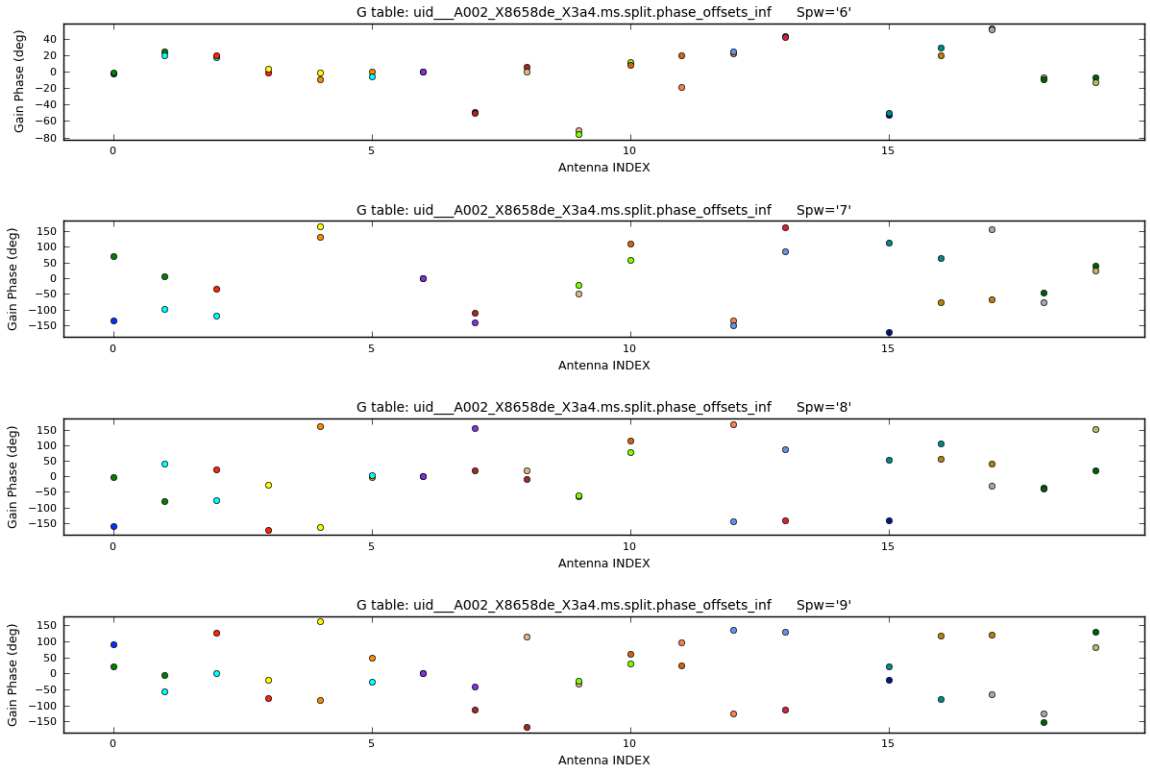

Figure 10: TDM-to-FDM phase offsets in Band 9 (X3a4) using (wide) SPW 0 as the reference. SPW 6 seems to “match” best, similar to the behavior in the other Band 9 TDM-to-FDM transfer.

Atacama Large Millimeter/
Submillimeter Array
Alonso de Córdova 3107
Vitacura - Santiago Chile

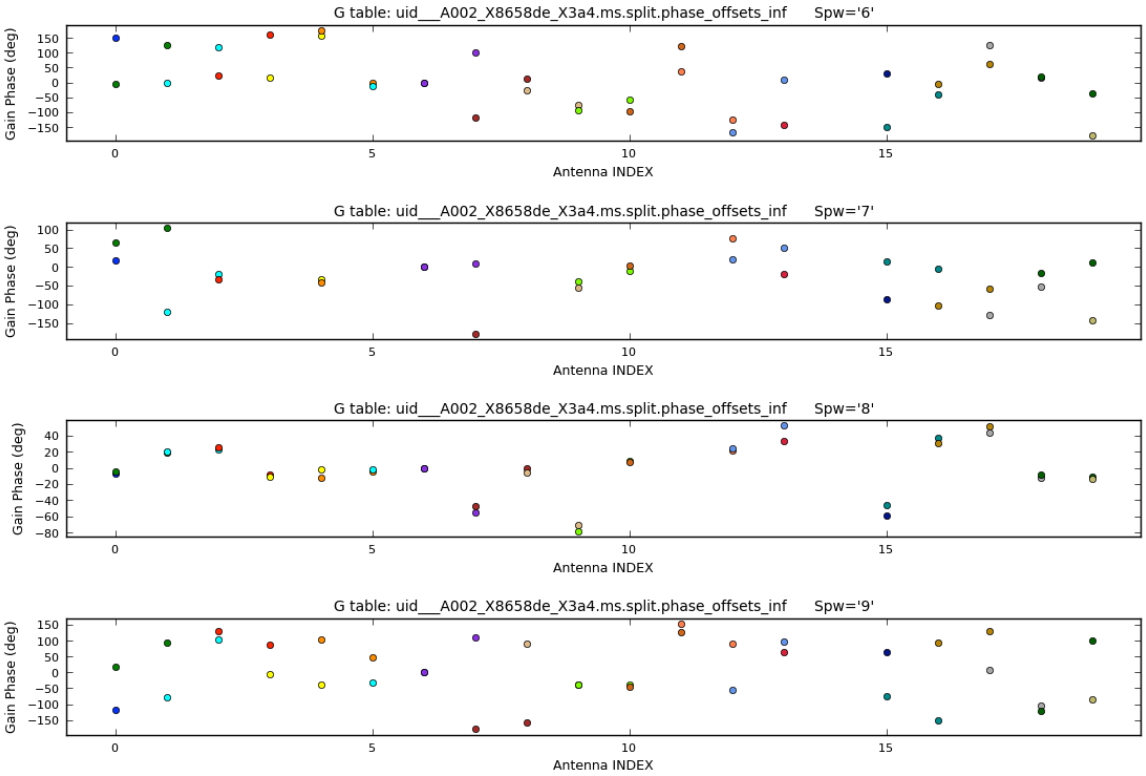

Figure 11: TDM-to-FDM phase offsets in Band 9 (X3a4) using SPW 2 as the reference. SPW 8 seems to “match” best, similar to the behavior in the other Band 9 TDM-to-FDM transfer.

Atacama Large Millimeter/
Submillimeter Array
Alonso de Córdova 3107
Vitacura - Santiago Chile

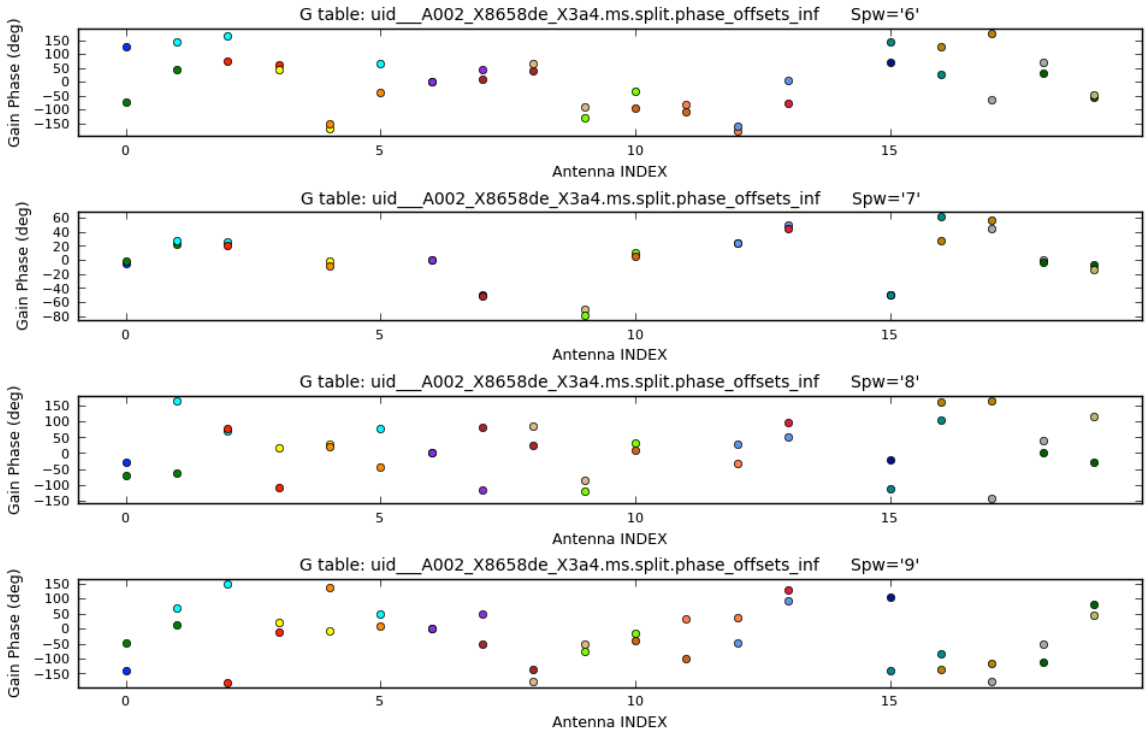

Figure 12: FDM-to-FDM phase offsets in Band 9 (X3a4) using SPW 4 as the reference. SPW 7 seems to "match" best, similar to the behavior in the other Band 9 TDM-to-FDM transfer.

Finally, instrumental phase offsets on individual antennas depend on the reference antenna specified as well as the observing frequency. They are not constant from one observation to another if the frequency changes even if the reference antenna is kept consistent. The offsets between the wide and narrow windows are also observed to change.

Future work and related testing:
Currently, testing is ongoing to determine the stability of the bandpass in the wide and narrow windows; these seem to be very stable, but recommendations may result from these tests indicating the best way to derive the narrow bandpasses, especially in the low signal to noise regime. One possibility is to use a more complicated bandpass solution fitting, like spline fitting (gaintype=BPOLY) or smoothing in real and imaginary space.

The usage of DiffGainCal will also be added soon to the observing setup for bandwidth switching (and band-to-band observing). This will enable quick switching back and forth between the wide and narrow bandpass calibrators. Depending on the needs of the band-to-band data reduction, the timing of the bandpass calibration within the SB may be different than it is currently, which is fine

for running bandwidth switching as long as enough signal-to-noise can be achieved in the narrow bandpass observations. The usage of DiffGainCal will be testable soon.

Additionally, a new observing strategy will soon be implemented in the automatic script generator for flux calibration transfer between the flux and bandpass calibrators. This will affect the way that the amplitude calibration is done in bandwidth switching data reductions.

Finally, this method should be combined with the band-to-band transfer method of high frequency calibration once both are adequately characterized on their own. The addition of the DiffGainCal to the observing strategy and new flux/bandpass calibration data reduction strategy will be necessary to combine these techniques.

Summary:
-- Bandwidth switching from TDM to FDM windows within the same frequency band is a viable way to calibrate high frequency observations; it has been demonstrated in B3, B7, and B9.

-- Wide FDM window to narrow FDM window phase solution transfer can also be used; this does not appear to perform better than the TDM transfer (in the X3a4 B9 scheduling block).

-- Alterations to the automatically generated script are described. The usage of 'linearPD' should be avoided (though it appears to only make a 1-2% difference in the final image rms).

-- Suggestions to improve the observing setup (using solar system objects, taking an extra bandpass calibration) are described and testing fixes to the documented phase decorrelation and target numbering problems are recommended, as is testing in various conditions to determine the limits of bandwidth switching capabilities.

-- Including a bandpass measurement in the narrow windows improves the final image in Bands 3 and 7. In Band 9, the SNR is similar regardless of the inclusion of a narrow window bandpass calibration (though this should be tested in data taken with better weather). In the same Band 9 SB, including the WVR correction increases the rms in the final image by 20% but does a better job of recovering flux at the phase center than the "no WVR" case, though the "no WVR" case finds the target closer to its true location on the sky.

-- Position offsets are seen in all of the final images ranging from 10% of the beam (B3, B9) to 100% of the beam (B7). In the B9 "no WVR" case, the offset is halved compared to the offset seen with the WVR applied; the weather was fairly bad in this observation. In the FDM-to-FDM transfer B9 data, the offset is smaller than the TDM-to-FDM transfer, though they are both quite small (7-11% of the beam size).

-- Phase offsets are measured between the wide TDM and narrow FDM windows when the wide windows do not overlap and have a one-to-one correspondence with the narrow windows. For an individual antenna, the offsets change with SPW and frequency band (and reference antenna). In Band 3, the magnitude of the offsets is roughly ±10 degrees, and in Bands 7 and 9, the offsets are roughly ±40-50 degrees. In Bands 3 and 7, the offsets in the two polarizations are within ~5 degrees of each other; this proximity is not always seen in Band 9, regardless of the weather.

-- Phase offsets are measured in Band 9 between TDM and FDM windows, as well as between wide FDM and narrow FDM windows, when the wide windows all have the same central frequency. In this case, depending on which TDM/wide FDM window is used as the reference, one of the narrow FDM windows exhibits the roughly ±40 degree behavior seen previously. The rest of the narrow windows exhibit up to ±160 degree offsets; there appears to be one “matching” narrow SPW in each case.

-- Instrumental phase offsets on individual antennas depend on the reference antenna specified as well as the observing frequency. They are not constant from one observation to another if the band changes even if the reference antenna is kept consistent.

-- Related testing is summarized (bandpass stability), as is future work, including the usage of DiffGainCal, an update to the method to be used in the script generator, and the (eventual) combination of this technique with the Band-to-Band transfer technique.